Cancer Letters 297 (2010) 231–243

Contents lists available at ScienceDirect

Cancer Letters

journal homepage: www.elsevier.com/locate/canlet

A small oxazine compound as an anti-tumor agent: A novel pyranoside mimetic that binds to VEGF, HB-EGF, and TNF-α

Basappa [a,b,d,e,1,2], Sengottuvelan Murugan [a,1,2], Chandagirikoppal V. Kavitha [c], Anurag Purushothaman [b], Kottayath G. Nevin [a], Kazuyuki Sugahara [a,b], Kanchugarakoppal S. Rangappa [c,*]

[a] Laboratory of Proteoglycan Signaling and Therapeutics, Faculty of Advanced Life Science, Hokkaido University Graduate School of Life Science, Sapporo, Japan
[b] Department of Biochemistry, Kobe Pharmaceutical University, Kobe, Japan
[c] Department of Studies in Chemistry, University of Mysore, Mysore, India
[d] Singapore-MIT Alliance for Research and Technology (SMART), Centre for Life Sciences, S16-05-06, 28 Medical Drive, Singapore 117456, Singapore
[e] Department of Chemistry, Bangalore University, Bangalore, India

ARTICLE INFO

Article history:
Received 2 February 2010
Received in revised form 17 May 2010
Accepted 25 May 2010

Keywords:
Tumor metastases
Heparin
Growth factors
Oxazines
Sugar mimetics

ABSTRACT

A novel pyranoside mimetic compound, DMBO (2-(2,6-difluorophenyl)-5-(4-methoxyphenyl)-1-oxa-3-azaspiro[5.5]undecane), was designed and synthesized. The sugar mimicking behavior of DMBO was addressed by its ability to bind several growth factors/cytokines such as vascular endothelial growth factor (VEGF), heparin-binding epidermal growth factor-like growth factor (HB-EGF), and tumor necrosis factor (TNF)-α as demonstrated by the recently developed surface plasmon resonance assay. DMBO exhibited strong anti-proliferation activity *in vitro* against tumor cells including a highly metastatic murine osteosarcoma cell line LM8G7 that secretes VEGF as well as two human ovarian cell lines, OVSAHO and SKOV-3, which secrete TNF-α and HB-EGF respectively. Furthermore, DMBO inhibited the metastatic activity to the mouse liver of LM8G7 cells injected from a lateral tail vein, and affected the heparan-degrading activity of LM8G7 cells. Here, we report that DMBO acts as a human heparanase inhibitor *in vitro* possibly as a substrate mimetic. DMBO also inhibited the migration and invasion of LM8G7 cells and angiogenic events such as endothelial cell proliferation, migration and capillary tube-like formation *in vitro*. More prominently, the administration of DMBO with heparin resulted in synergistic anti-tumor effects in mouse model of osteosarcoma. These preclinical data shows the potential anti-cancer effects of DMBO.

1. Introduction

Synthetic heterocyclic compounds have been used extensively for drug development and the treatment of diseases including cancer [1]. Among them, oxazines are well known for their potential biological effects, for example, the inactivation of chymotrypsin by 5-butyl-3*H*-l,3-oxazine-2,6-dione [2]. In addition, 5-β-D-ribofuranosyl-l,3-oxazin-2,4-dione, a C-ribonucleoside antibiotic (minimycin), is used as an anti-tumor agent [3] and 5-methyl-3*H*-1,3-oxazine-2,6-dione is used as a suicide inactivator of serine

Abbreviations: DMBO, (2-(2,6-difluorophenyl)-4a,5,6,7,8,8a-hexahydro-4a-(4-methoxyphenyl)-4H-benzo[e][1,3]oxazine); HS, heparan sulfate; VEGF, vascular endothelial growth factor; HB-EGF, heparin-binding epidermal growth factor-like growth factor; TNF-α, tumor necrosis factor-α; DMEM, Dulbecco's Modified Eagle's Medium; FBS, fetal bovine serum; rh, recombinant human; SPR, surface plasmon resonance; DMSO, dimethyl sulfoxide.

* Corresponding author. Address: Department of Studies in Chemistry, University of Mysore, Manasagangotri, Mysore 570 006, India. Tel./fax: +91 821 2412191.
E-mail address: rangappaks@gmail.com (K.S. Rangappa).

[1] These authors contributed equally.

[2] Supported by a postdoctoral fellowship from the JSPS.

0304-3835/$ - see front matter © 2010 Elsevier Ireland Ltd. All rights reserved.
doi:10.1016/j.canlet.2010.05.016

proteases [4]. In the search for an effective therapeutic agent for cancer, which targets multiple pathways, we designed and synthesized a novel six-membered oxazine compound, DMBO (2-(2,6-difluorophenyl)-4a,5,6,7,8,8a-hexahydro-4a-(4-methoxyphenyl)-4*H*-benzo[e][1,3]oxazine), a class of sugar mimetic, in which the ring carbon has been replaced by a nitrogen atom. The oxazine nucleus of the DMBO is appeared to mimic the pyranoside ring structure, which is the monosaccharide back bone of the sugar residues in the heparan sulfate (HS).

HS on cell surfaces modulates signal transduction to tumor cells by interacting with various growth factors such as fibroblast growth factor-2 [5], vascular epidermal growth factor (VEGF) [6], and heparin-binding epidermal growth factor-like growth factor (HB-EGF) [7]. Cell-surface and extracellular matrix HS plays a major role in tumor metastasis, and acts as a storage shed for various proteins [8]. Heparanase, an endo-β-D-glucuronidase family member, promotes tumor cell invasion by degrading HS in the extracellular matrix [9,10]. Heparanase promotes cell proliferation, metastasis and angiogenesis by releasing growth factors such as fibroblast growth factor-2 and VEGF from HS [11,12]. Several studies have shown that HS mimetics act as anti-tumor agents. For example, anti-tumor and anti-heparanase activities of a non-sugar-based HS mimetic compound KI-105 have been reported [13].

In addition to the matrix components and matrix-degrading enzymes, malignant cells produce a variety of soluble factors such as VEGF, HB-EGF, and tumor necrosis factor-α (TNF-α), which play a major role in tumor progression. Heparin-binding growth factors like fibroblast growth factor-2, VEGF and HB-EGF have been implicated in the metastatic process [14]. VEGF plays a major role in both vasculogenesis and angiogenesis by triggering a tyrosine kinase pathway [15]. Some members of the VEGF family stimulate cellular responses by binding to cell-surface heparan sulfate proteoglycans as co-receptors [16]. Therefore, effective VEGF antagonists or the VEGF receptor agonists that mimic HS may be good tools to inhibit VEGF production. HB-EGF activates at least three signal transduction pathways, which are involved in proliferation, the secretion of VEGF, and the stimulation of chemotaxis in cancer cells [17]. The expression of ligands for the EGF receptor, such as transforming growth factor-α is also often increased in gliomas, resulting in an autocrine loop that contributes to the growth autonomy of glioma cells [18]. Importantly, HB-EGF and EGF act downstream by binding to EGF receptor on the cell surface with high affinity [19]. Therefore, it is reasonable to expect either inhibition of the expression of HB-EGF or blocking of the EGF receptor pathway to have therapeutic value in the treatment of a variety of cancers. This notion is consistent with the finding that neutralizing antibodies against HB-EGF blocked the transactivation of EGF receptor and inhibited the tumor growth in mice [20]. Increasing evidence shows that TNF-α acts as a key mediator for local inflammation and also in the development of cancer, suggesting that anti-TNF-α therapy might be effective against pancreatic tumor growth and metastasis [21].

DMBO mimics the pyranosidic ring structure of HS. Here, we demonstrate DMBO's ability to bind various growth factors/cytokines such as VEGF, HB-EGF, and TNF-α and also presented the anti-tumor activity of DMBO with heparin synergistically.

2. Materials and methods

2.1. Synthesis of DMBO

Equimolar 2,6-difluoro benzaldehyde (0.44 g) was added to a solution of 1-[2-amino-1-(4-methoxy-phenyl)-ethyl]-cyclohexanol monoacetate (1.0 g, 3.13 mmol) in 5.0 mL of methanol in the presence of anhydrous K_2CO_3 (1.3 g, 10 mmol) and the reaction mixture was stirred at room temperature for 10–12 h to obtain DMBO. Dry weight: 0.85 g, yield: 85%, m.p. 102 °C. The analytical grade compound was obtained by recrystallization using methanol as a solvent (6 mL). The product was confirmed by IR, ^{1}H NMR and elemental analysis. ^{1}H NMR (400 MHz, $CDCl_3$): δ_H 0.75–0.93 (t, 2H, cyclohexyl); 1.1–1.6 (m, 6H, cyclohexyl); 2.48–2.65 (t, 2H, cyclohexyl); 3.32 (s, 1H, –NH–); 3.47–58 (t, 2H, N–CH_2–); 3.64–3.73 (s, 3H, O-CH_3); 3.78–3.82 (t, 1H, –CH–Bz–O–CH_3); 5.67–5.69 (br d, 1H, –CH–Bz); 6.75–6.90 (d, J = 16 Hz, 2H, Ar–H); 7.05–7.18 (d, J = 8 Hz, 4H, Ar–H); 7.3–7.5 (m, 1H, Ar–H). Anal. ($C_{22}H_{25}F_2NO_2$) C, H, N. Molecular weight: 373.4 Da. The melting points were determined on a SELACO-650 hot stage apparatus and are uncorrected. ^{1}H NMR were recorded on a Shimadzu AMX 400 spectrometer by using $CDCl_3$ as solvent and TMS as an internal standard (Chemical shift in ppm). Elemental analyses were obtained on a vario-EL instrument and were within ±0.4% of calculated values.

2.2. X-ray crystallographic study of DMBO

A single crystal of DMBO of good quality was obtained by slow evaporation using methanol as a solvent at room temperature. The crystal ($0.25 \times 0.2 \times 0.2$ mm) was selected after optical microscopic examination. X-ray diffraction intensity was measured by ω scans using a DIPlabo 32001 diffractometer attached to a CCD area detector and a graphite monochromator for Mo Kα radiation (50 kV, 40 mA). A hemisphere of reciprocal space was collected using the SMART software with the 2θ setting of the detector at 28°. Data reduction was performed using the SAINT program (Siemens). The phase problem was solved by direct methods, and the non-hydrogen atoms were refined anisotropically by means of the full matrix least-squares procedure using the SHELXL97 program (Siemens). All the hydrogen atoms were located using the difference Fourier method. The absolute structure of DMBO is shown (Fig. 1C). Crystallographic data for the structural analysis have been deposited at the Cambridge Crystallographic Data Centre, CCDC-272761 for DMBO.

2.3. Biological materials

Nine-week-old female C3H/HeN mice and 10-week-old male C57BL/6 mice were obtained from Japan SLC (Hamamatsu, Japan) and kept in standard housing. All

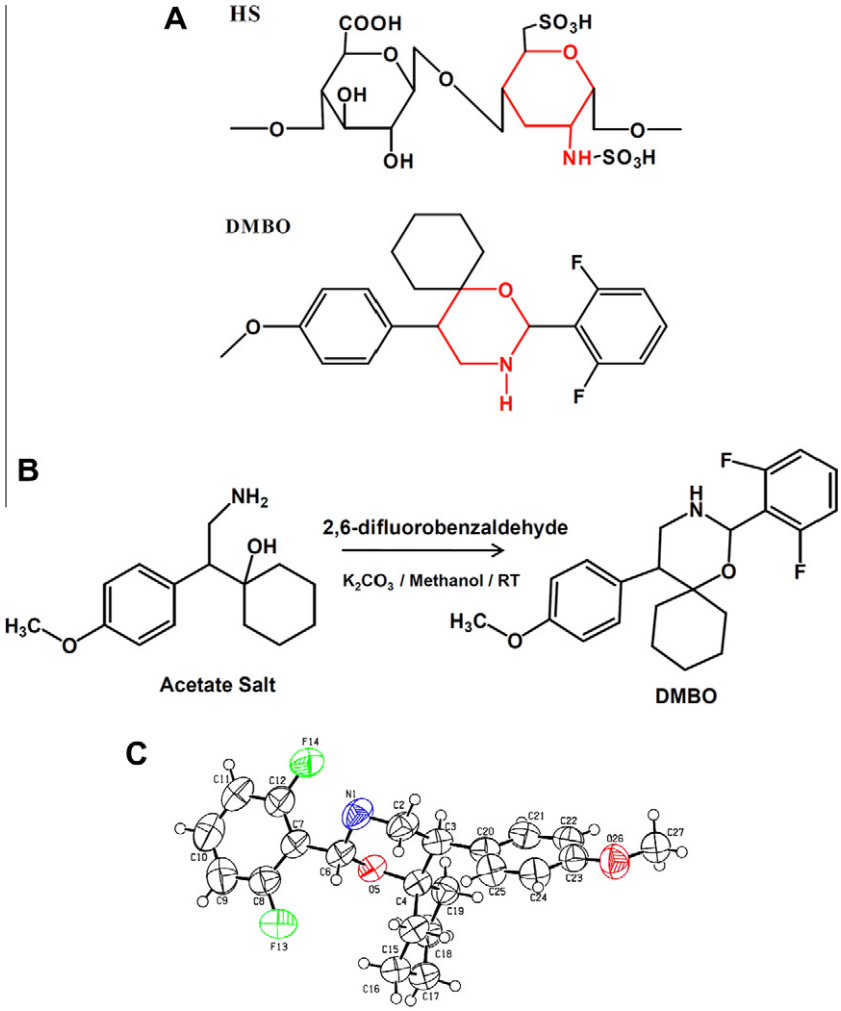

Fig. 1. Synthesis and crystal structure of a novel HS mimetic DMBO. (A) The comparison of the pyranose ring of the HS disaccharide unit and its mimetic oxazine ring of DMBO. (B) Schematic diagram for the synthesis of DMBO. (C) X-ray crystal structure of DMBO showing the Oak Ridge Thermal Ellipsoid Plot view. The *color coding* of the atoms is as follows: *black*, carbon; *dark blue*, nitrogen; *red*, oxygen; *light green*, fluorine; *small black circles*, hydrogen. (For interpretation of the references to color in this figure legend, the reader is referred to the web version of this article.)

the experiments were performed according to a protocol approved by the local animal care committee of Hokkaido University. LM8G7, a highly metastatic murine osteosarcoma cell line with the potential to form tumor nodules in the liver, was cloned from LM8G5 cells [22] as described [23,24] and cultured in Dulbecco's Modified Eagle's Medium (DMEM) supplemented with 10% (v/v) fetal bovine serum (FBS) (Thermo Trace, Melbourne, Australia), streptomycin (100 μg/mL), penicillin (100 units/mL), 100× non-essential amino acids, β-mercaptoethanol (50 μM), 100× sodium pyruvate, and L-glutamine (2 mM) at 37 °C in a humidified 5% CO_2 atmosphere. The cells were harvested after incubation with 0.1% trypsin/1 mM EDTA in PBS for 5 min at 37 °C followed by gentle flushing with a pipette, and subcultured thrice a week. Human ovarian cancer cells (OVSAHO and SKOV-3) and mouse vascular endothelial cells (UV♀2) were purchased from RIKEN Cell Bank, Japan. The OVSAHO cells were cultured in RPMI medium supplemented with 10% (v/v) FBS, L-glutamine (2 mM), and $NaHCO_3$ (10%). The SKOV-3 cells were cultured in McCoy's 5A medium supplemented with 10% (v/v) FBS and L-glutamine (2 mM). The UV♀2 cells were maintained in DMEM supplemented with 10% (v/v) FBS. Bovine serum albumin (BSA), cisplatin, suramin, recombinant human HB-EGF (rh-HB-EGF), rh-HGF, rh-midkine, rh-TNF-α, rh-$VEGF_{165}$, and rh-pleotrophin were purchased from Wako Pure Chemicals Co. (Osaka, Japan). Mifepristone and lipopolysaccharide (LPS) were from Sigma (St. Louis, MO). All other chemicals and reagents used were of the highest commercial grade available.

2.4. Surface plasmon resonance (SPR) assay

To introduce DMBO and other small molecules onto a gold surface for SPR measurements, photo-affinity-linker-coated gold substrates were prepared. Briefly, a gold-coated glass chip (TOYOBO, Osaka, Japan) was immersed in a 0.5 mL ethanol solution, which contained 0.1 mM of the photo-affinity linker and 0.9 mM of a dummy linker for 12 h. The chip was rinsed successively with ethanol,

water and ethanol, and then dried to obtain a photo-reactive chip. The oxazines solution (10 mM in dimethyl sulfoxide (DMSO)) was spotted on the chip using an automated spotter (TOYOBO). The chip was dried in vacuo, and then irradiated at 365 nm under a UV transmission filter (Sigma-Koki, Japan) with a CL-1000L ultraviolet crosslinker (UVP Inc., CA). The chip was washed with DMSO for 12 h and then rinsed with ethanol. The oxazines-immobilized gold substrate was set into an SPR imaging instrument (TOYOBO), and each growth factor (50 μg/mL) in the running buffer (10 mM HEPES, 150 mM NaCl, pH 7.4) was injected onto the array surface at 0.1 mL/min and incubated for 10 min. All SPR experiments were performed at 30 °C. The interaction between the oxazines and the growth factors/cytokines such as VEGF, HB-EGF, TNF-α, FGF-2, midkine, pleotrophin and BSA were carried out using the SPR imaging instrument. The SPR image and signal data were collected with an SPR analysis program (TOYOBO). The SPR difference image was constructed by using the Scion Image program (Scion, MD).

2.5. Real-time proliferation assay

The cell proliferation assay was done using the RT-CES™ system (ACEA Biosciences, San Diego, CA). LM8G7 (5×10^3 cells/well) or OVSAHO (15×10^3 cells/well) cells were seeded in ACEA's 96X e-plate™ in a final volume of 150 μL [25]. Approximately 24 h after seeding, when in a log growth phase, the cells were incubated with 150 μL of DMEM containing various concentrations of DMBO (10–80 μM) or DMEM containing DMSO as a control. The effects of DMBO on the proliferation of LM8G7 or OVSAHO cells were monitored dynamically every 10 min. A cell index (quantitative measurement of cell proliferation) was plotted against time. The IC_{50} values were calculated from concentration–response curves by a non-linear regression analysis using the GraphPad Prism(GraphPad Prism Software Inc., San Diego, CA).

2.6. In vitro cell proliferation assay

SKOV-3 or UV♀2 cells were seeded at a density of 10×10^3 cells/well in a 96-well plate and incubated overnight at 37 °C. The SKOV-3 or UV♀2 cells were treated with DMBO for an additional 48 h or 72 h respectively. The final concentrations of DMBO used were (1, 17 or 195 μM) for SKOV-3 cells. Mifepristone (155 μM) or cisplatin (10 μM) was used as a positive control. The UV♀2 cells were treated with DMBO (1–59 μM) in the presence of VEGF (2 ng/mL) or DMBO (2–96 μM) alone in the absence of VEGF. In other instances, to investigate the specific effects of DMBO on VEGF-mediated cell proliferation, DMBO (50 μM) or heparin (100 μg/mL) were incubated with LM8G7 cells along with various concentration of exogenous VEGF (0–6 ng/mL) for 48 h and used for the experiment. In addition, to investigate the possible synergistic or additive effects of DMBO and heparin on the proliferation of LM8G7 cells, DMBO (25 or 50 μM) alone and heparin (25 or 50 μg/mL) alone or in combination of DMBO (25 or 50 μM) with heparin (25 or 50 μg/mL) was tested. The DMSO solution of DMBO was diluted with DMEM (150 μL) to yield a final concentration of 1–195 μM (final concentration of DMSO, <0.1%). The viability of control cells and cells treated with DMBO was measured using the Tetracolor One cell proliferation assay kit (Seikagaku Co., Tokyo, Japan). Absorbance at 450 nm was monitored to calculate the viability of the cells in percentage terms.

2.7. Liver metastasis assay

C3H/HeN mice were intravenously injected with 1×10^6 LM8G7 cells in 200 μL of serum-free DMEM via the lateral tail vein on day 0. Some mice received an intravenous injection of DMBO (0.25, 0.5, 1.0 or 1.5 mg/kg body weight) suspended in 200 μL of serum-free DMEM, on day 3, 5 and 10 after the tumor cell injection. After 4 weeks, the mice were sacrificed, the number of liver nodules was counted macroscopically, and liver weight was measured in the control and DMBO-treated animals. Heparin (2.5 or 5.0 mg/kg body weight) alone was used, as a positive control. The possible synergistic or additive effects of DMBO and Heparin were investigated by subsequent administration of DMBO (0.25 or 0.5 mg/kg body weight) and heparin (2.5 or 5.0 mg/kg body weight) as described above.

2.8. Heparanase activity assay

Human heparanase activity *in vitro* was determined using fluorescein isothiocyanate (FITC)-HS as the substrate, as described previously [26]. The reactions were carried out in the presence or absence of DMBO (28, 58, 78, 100 or 118 μM) in 100 μL of 0.1 M sodium acetate buffer, pH 4.2, containing 1 μg of FITC-HS, at 37 °C for 3 h and terminated the reaction by heating at 100 °C for 5 min. The reaction mixture was centrifuged at 15,000 rpm for 5 min to precipitate the insoluble material. The products of FITC-HS yielded by this reaction were analyzed by gel-permeation chromatography. Briefly, a 20-μL aliquot of the supernatant was injected into a TSKgel G3000SWXL column (Tosoh Biosciences, Montgomeryville, PA) equilibrated with column buffer (25 mM Tris–HCl, 150 mM NaCl, pH 7.5) at a flow rate of 1 mL/min. The activity was determined from HPLC chromatograms by measuring a forward half area of the peak of the intact FITC-HS. The decrease of the peak area observed following heparanase treatment was measured by using an integrator, and the amount of the degraded FITC-HS was calculated from the decrease in fluorescence intensity. One unit was defined as the quantity of the enzyme that degraded 10 ng of FITC-HS/min. Suramin (50 μM), a heparanase antagonist was used a positive control.

2.9. In vitro heparan-degrading assay

LM8G7 (1×10^6) cells were seeded into a 6-well plate and incubated overnight. After 24 h, the cells were incubated with DMBO at concentrations of 55, 104, and 206 μM in triplicate. To determine the effect of DMBO on the heparan-degrading activity of LM8G7, the cells were further incubated for 48 h at 37 °C. The cells were collected by centrifugation, and a whole-cell lysate was prepared as reported [27]. Protein concentrations of the samples were

determined using a BCA (bicinchoninic acid) assay kit (Thermo Fisher Scientific Inc., Rockford, IL), and adjusted to 0.1 mg/mL. The heparan-degrading activity in DMBO-treated/untreated cell lysates was measured using a Heparan Degrading Enzyme Kit (Takara, Ootsu, Japan).

2.10. Cell migration and invasion assays in vitro

The migration or invasion of LM8G7 cells was assessed using BD BioCoat™ chamber with or without Matrigel (BD Biosciences) *in vitro*. Briefly, single cell suspensions of LM8G7 (2×10^5 cells/mL) were prepared by detaching and resuspending the cells in DMEM. Before the cells were added, the chambers were rehydrated for 2 h in an incubator at 37 °C. The lower chambers were filled with DMEM containing 10% FBS. After the addition of the cells with or without DMBO (0.5–5 μM) to the upper chamber, the chambers were incubated for a further 8 h at 37 °C. The cells that had not migrated or invaded were removed from the upper surface of the membrane by scrubbing. The cells that had migrated or invaded through and remained bound to the underside of the filter were fixed, stained with a Diff-Quick solution, and counted in five random fields per filter. Images of migrated cells were captured by a phase contrast microscope (Olympus, IX70, Japan). The number of migrated or invaded cells in the presence or absence of DMBO was counted.

2.11. Migration of UV♀2 cells in a wound closure model

UV♀2 cells were seeded in a 6-well plate and allowed to grow to complete confluence. Subsequently, a plastic pipette tip was used to scratch the cell monolayer to create a cleared area, and the wounded UV♀2 cell layer was washed with a fresh medium to remove loose cells, and photographed using CKX41 Olympus microscope (Olympus, Japan) equipped with 10× objective lenses. The cells were incubated with or without DMBO (0.5 or 1 μM) along with 2 ng/mL VEGF, and the inhibition of the wound healing by DMBO was photographed after 8 h incubation.

2.12. In vitro angiogenesis assay

ECMatrix™ (Chemicon, CA) was added to a 96-well plate in a final volume of 100 μL and allowed to solidify at 37 °C for 30 min. Single cell suspensions of UV♀2 cells (100 μL) were seeded at a density of 4×10^5 cells/mL to the ECMatrix™-coated wells with or without the indicated concentrations of DMBO (0.5 or 1 μM) along with 2 ng/mL VEGF. After 8 h of culture, the reorganization of the sub-confluent monolayer of UV♀2 cells in 3-dimensional ECMatrix™ was monitored and photographed under an Olympus FX380 microscope attached to a 3CCD camera. The number of tubes present in each well was counted and averaged.

2.13. Statistical analysis

The statistical analysis was done using a software Origin 8 (OriginLab). The Mann–Whitney *U* test was used to determine *P*-values.

3. Results and discussion

Heparin and most of the HS mimetics that act to enhance the inhibition of inflammation and tumor metastasis are sulfated oligosaccharides (e.g., heparin derivatives, laminarin sulfate, and chitin derivatives) [28–30]. Low molecular weight HS mimetics which perform multiple biological functions *in vivo* and *in vitro* with high specificity are rare. Among HS mimetics, PI-88 (phospho mannopentaose) has been reported as an anti-tumor agent, which significantly inhibits tumor growth, metastasis, and angiogenesis [31]. An HS mimicking a pseudodisaccharide has been reported as an inhibitor of heparanase [32]. All these compounds have a

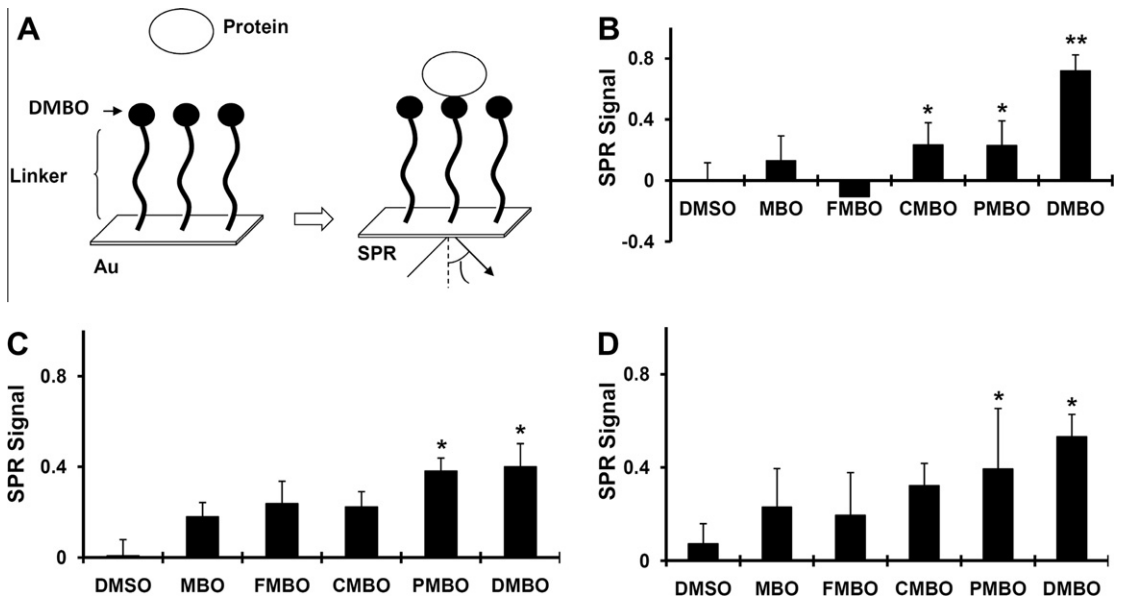

Fig. 2. Interaction between DMBO and growth factors/cytokines. Overview of the SPR analysis (A). DMBO (10 mM) was immobilized on the photo-affinity-linker-coated gold substrates. Interactions were detected between DMBO and the growth factors/cytokines in solution by SPR imaging; B–D, the maximum SPR signal strength observed by DMBO and VEGF (B), TNF-α (C), or HB-EGF (D). $^{*}P < 0.05$ versus control. $^{**}P < 0.01$ versus control. Mann–Whitney *U* test.

sugar-based structure, and this has endowed us with an inspiration to synthesize a novel non-sugar-based compound, DMBO, which appears to mimic the functional groups and pyranoside ring structure present in HS in the form of monosaccharide backbone (Fig. 1A).

3.1. Synthesis of DMBO

The DMBO was prepared by the cyclization of 1-[2-amino-1-(4-methoxy-phenyl)-ethyl]-cyclohexanol monoacetate [33,34] with 2,6-difluoro benzaldehyde in the presence of potassium carbonate (Fig. 1B). Further, we obtained DMBO in single crystalline form (Fig. 1C).

3.2. Examination of the binding of DMBO to growth factors and chemokines

In recent years, many high-throughput methodologies have been developed to identify potential anti-cancer molecules [28]. In view of the fact that, the synthesized compounds appeared to mimic the pyranoside ring structure of HS; we expected that these compounds should have binding ability with heparin-binding growth factors and they must display some characteristics common to those of some well known HS mimetic molecules. We conducted a novel SPR assay to screen the ability of small molecules (around 69 molecules) to bind various growth factors/cytokines such as VEGF, HB-EGF, and TNF-α which are thought to

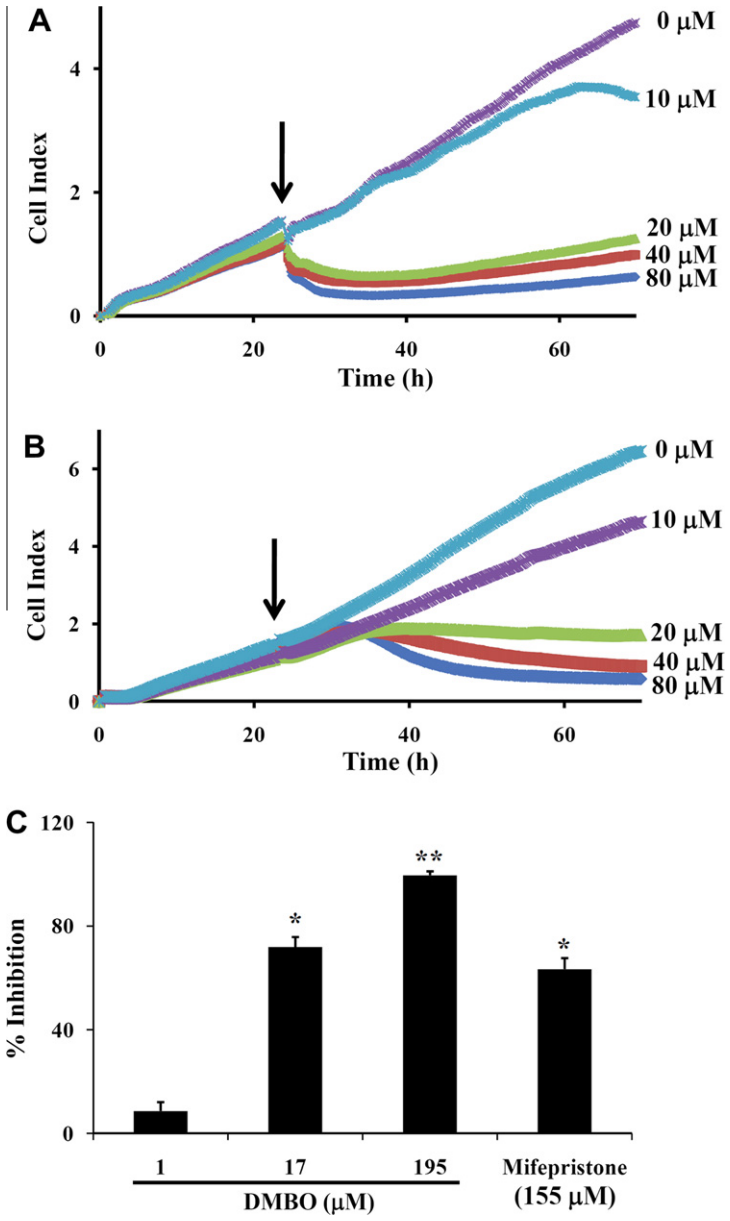

Fig. 3. Effects of DMBO on the proliferation of cancer cells. (A) Real-time monitoring of the effects of DMBO on the proliferation of LM8G7 cells. LM8G7 cells were seeded in ACEA's 96X e-plate™ at a density of 5×10^3 cells per well, and continuously monitored using the RT-CES system up to 24 h, at which point DMBO (10–80 μM) was added. The cell index is plotted against the time. (B) Real-time monitoring of the effects of DMBO on the proliferation of OVSAHO cells. OVSAHO cells were seeded in ACEA's 96X e-plate™ at a density of 15×10^3 cells per well and DMBO was added as described above. The arrow indicates the time of the addition of DMBO. Data represent the mean values ± S.D. for three identical wells from three independent experiments. (C) % Inhibition of DMBO against the proliferation of SKOV-3 cells. SKOV-3 cells were cultured overnight and incubated with or without the indicated concentrations of DMBO (1, 17 or 195 μM) or mifepristone (155 μM). The total number of viable cells was determined and the % inhibition of DMBO against the proliferation of SKOV-3 cells was presented.

be involved in the progression of cancer. Recently we improved our photo-affinity SPR imaging technique by reviewing the thiol linkers used to coat the surface of the gold substrate [35]. A new photo-affinity linker (Supplemental Fig. 1) improved the sensitivity with which the interaction between small molecules and proteins was detected, and allowed the detection of the direct binding of growth factors/cytokines to small molecules. An overview of the SPR analysis is shown in Fig. 2A. DMBO and other screened small molecules were immobilized on the photo-affinity-linker-coated gold substrates. In our *in vitro* experimental conditions, strong to moderate SPR signals for the direct binding of DMBO with VEGF, TNF-α and HB-EGF were found (Fig. 2B–D and Supplemental Figs. 2–4).

We demonstrated here that DMBO interacted significantly with VEGF, TNF-α, and HB-EGF directly as detected by SPR assay, when compared to other compounds synthesized (Supplemental Scheme 1). The SPR signal of DMBO was significantly stronger than that of other structurally similar compounds having the same oxazine nucleus (Fig. 2B–D). We compared the binding specificity of DMBO to the growth factors/cytokines with the similar scaffold molecule, which bearing different substitution at the second position of the oxazine nucleus. The compounds like 4a,5,6,7,8,8a-hexahydro-4a-(4-methoxyphenyl)-4*H*-benzo[e][1,3]oxazine (MBO); 2-(4-fluorophenyl)-4a,5,6,7,8,8a-hexahydro-4a-(4-methoxyphenyl)-4*H*-benzo[e][1,3]oxazine (FMBO); 2-(4-chlorophenyl)-4a,5,6,7,8,8a-hexahydro-4a-(4-methoxyphenyl)-4*H*-benzo[e][1,3]oxazine (CMBO) and 2-(3-Pyridyl)-4a,5,6,7,8,8a-hexahydro-4a-(4-methoxyphenyl)-4*H*-benzo[e][1,3] oxazine (PMBO) were interacted with the growth factors/cytokines weakly when compared to DMBO (Fig. 2B–D). This indicates that the 2,6-difluorophenyl group of DMBO is important for the strong interaction with VEGF, TNF-α, and HB-EGF and very weakly with FGF-2 (Supplemental Fig. 5). DMBO did not bind to other heparin-binding growth factors such as pleiotrophin and midkine (Supplemental Figs. 6 and 7). These results indicate that the compound DMBO binds more specifically towards VEGF and led us to speculate that DMBO may be used to modulate the VEGF-mediated cellular pathways. However, the molecular mechanism of DMBO binding with these growth factors is unknown at this point. In addition, DMBO interacted with BSA (Supplemental Fig. 8) when compared to other structurally similar molecules, encourages the development of BSA–DMBO composite drug carrier systems for cancer therapeutic studies like many anti-cancer drugs in the near future. It has been shown that albumin plays an increasing role as a drug carrier *in vivo* to a great number of therapeutic drugs such as penicillins, sulfonamides, and indole compounds [36].

3.3. Effects of DMBO on the proliferation of growth factors secreting cancer cells

Arrest of tumor cell proliferation in the target organ is the ultimate objective of anti-cancer therapy [37]. To validate the direct binding ability of DMBO with the growth factors/cytokines and to know the biological effects, we investigated the anti-proliferative effect of DMBO on tumor cells, which are known to secrete the growth factors/cytokines endogenously. Initially, we examined the effect of DMBO on the proliferation of LM8G7 cells. DMBO (10–80 μM) inhibited the proliferation of

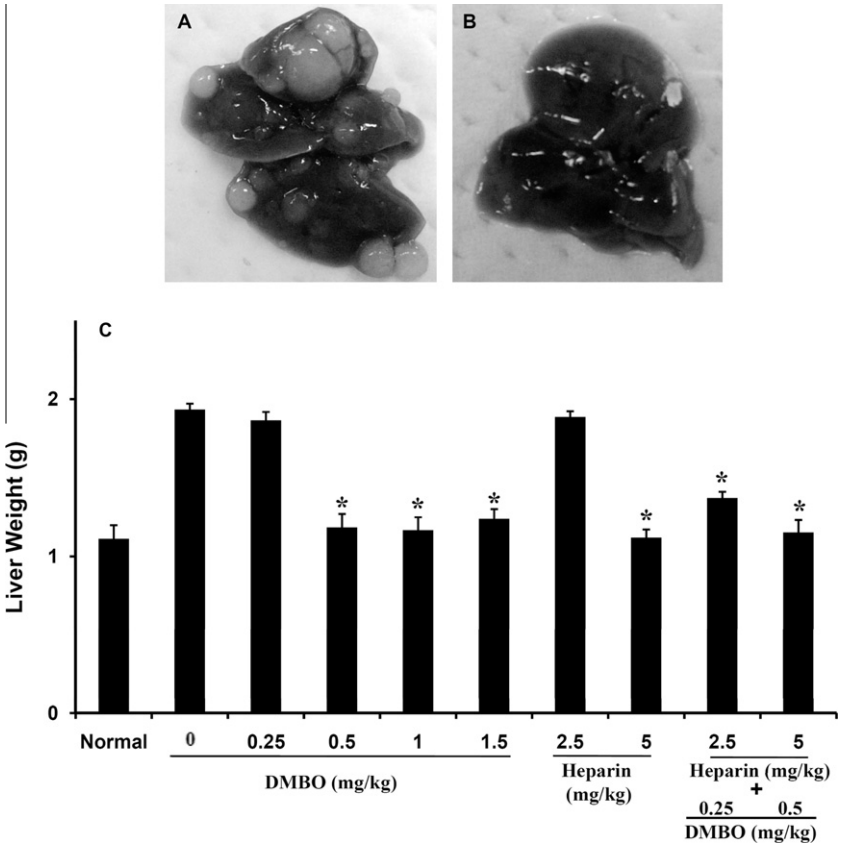

Fig. 4. Effects of DMBO against the metastatic potential of mouse osteosarcoma cells. C3H/HeN mice were intravenously injected with 1×10^6 LM8G7 cells in 200 μL of DMEM via the tail. Some mice received an intravenous injection of DMBO (0.25, 0.5, 1.0 or 1.5 mg/kg body weight) on day 3, 5 and 10. After 4 weeks, the mice were sacrificed, the number of liver nodules was counted macroscopically, and the liver weight was measured in the control and DMBO-injected animals. Representative livers from mice injected with LM8G7 cells treated with DMEM (A) and DMBO (0.5 mg/kg body weight) (B) are shown. The average liver weight of the control and the DMBO treated mice (C). Heparin from porcine intestinal mucosa was used as a positive control. The possible synergistic or additive effects of DMBO and heparin were investigated by subsequent administration of DMBO (0.25 mg/kg body weight) and heparin (2.5 mg/kg body weight) or DMBO (0.5 mg/kg body weight) and heparin (5.0 mg/kg body weight) as described above. Data represent mean values ± S.D. for three independent experiments and each experiment was conducted with six mice per group. $^*P < 0.05$ versus control. Mann–Whitney *U* test.

VEGF-expressing LM8G7 cells dose-dependently (Fig. 3A) with an IC_{50} value of 13 μM. Further, DMBO also inhibited the proliferation of TNF-α-expressing OVSAHO cells (Fig. 3B) with an IC_{50} value of 16 μM. In addition, DMBO at 195 μM completely inhibited (99%) the proliferation of HB-EGF expressing SKOV-3 cells, whereas mifepristone, a positive control, at 155 μM had a lesser effect (63%) (Fig. 3C). The compounds like MBO, FMBO, CMBO, or PMBO inhibited the proliferation of tumor cells to a lesser extent, when compared to DMBO (Supplemental Table 1). Interestingly, DMBO did not induce apoptosis on these cells (data not shown).

3.4. DMBO prevents liver metastasis in vivo

Inhibition of metastasis represents an attractive approach to the treatment of highly malignant tumors [38]. Mice given an intravenous injection of LM8G7 cells developed copious metastatic nodules in the liver within 30 days (Fig. 4A). In our dose fixation study, to elucidate the effective dose of DMBO or heparin, we used several concentration of DMBO (0.25, 0.5, 1.0 or 1.5 mg/kg body weight) alone or heparin (2.5 or 5.0 mg/kg body weight) alone. Our *in vivo* study revealed that DMBO at the concentration of 0.25 mg/kg body weight and heparin 2.5 mg/kg body weight had no anti-tumor effect. In contrast, mice treated intravenously with DMBO at 0.5, 1.0 or 1.5 mg/kg body weight were completely free of metastatic nodules in the liver (Fig. 4B). Moreover, we did not note any significant advantage provided by the 1.0 and 1.5 mg/kg body weight dose over the 0.5 mg/kg body weight dose, hence the minimal effective dose of DMBO was considered to be 0.5 mg/kg body weight.

Measurements of liver weight, which reflects tumor burden, gave similar results, with DMBO almost completely suppressing the increase in liver weight by inhibiting the formation of tumor nodules (Fig. 4C). The animals tolerated the dosages of DMBO well, showing no signs of tox-

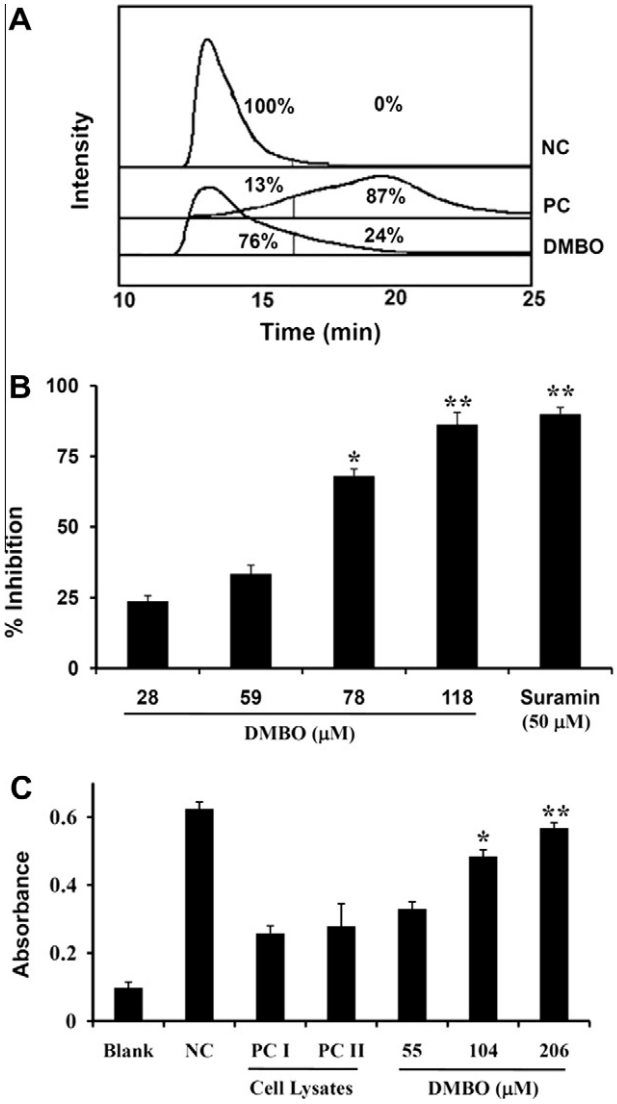

Fig. 5. Inhibitory effects of DMBO against the catalytic activity of heparanase. (A) The inhibitory action of DMBO (100 μM) on heparanase-mediated degradation of the FITC-HS substrate, using gel filtration HPLC degradation of FITC-HS were monitored by the fluorescence intensity as described previously [26] with excitation and emission wavelengths of 490 and 520 nm respectively. When compared to negative control (NC, the uninhibited heparanase), the decrease in the forward half area of FITC-HS following suramin treatment (PC), and the inhibition of heparanase activity by DMBO (100 μM DMBO) was calculated. (B) Overall inhibition rates of DMBO (28, 58, 78, 100 or 118 μM) on heparanase activity in the cell-free system. (C) Mean absorbance of the intact HS remaining after the incubation of LM8G7 cell lysates in the presence or absence of DMBO is shown. The adhered LM8G7 cells were treated with DMBO at the indicated concentration (55, 104 or 206 μM). Using the cell lysates, the heparan-degrading activity was determined. The negative control (NC) contained the substrate but no cell lysate. PC I and PC II, positive controls I and II. Data represent mean values ± S.D. for three independent experiments. $^{*}P < 0.05$ versus control. $^{**}P < 0.01$ versus control. Mann–Whitney *U* test.

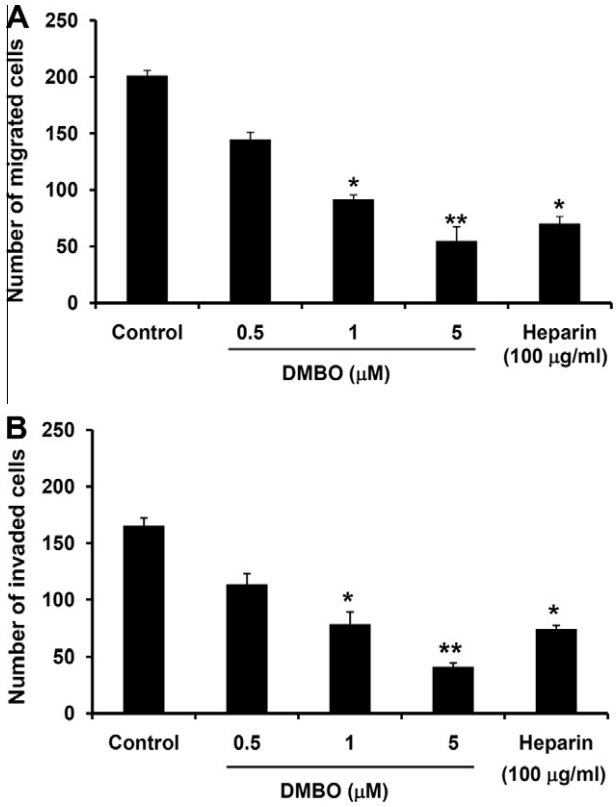

Fig. 6. Effects of DMBO against the migration and invasion of LM8G7 cells. LM8G7 cells were plated on BD BioCoat™ chambers (BD Biosciences) in the presence of fetal bovine serum. The cell migration (without Matrigel coat) and invasion (with Matrigel coat) were measured as described under "Experimental Procedures." Effects of DMBO (0.5–5 μM) or heparin (100 μg/mL) on the migration (A) and invasion (B) of LM8G7 cells measured as described under "Experimental Procedures." The data represent the mean value ± S.D. for two independent experiments. $^{*}P < 0.05$ versus control, $^{**}P$ 0.01 versus control, Mann–Whitney *U* test.

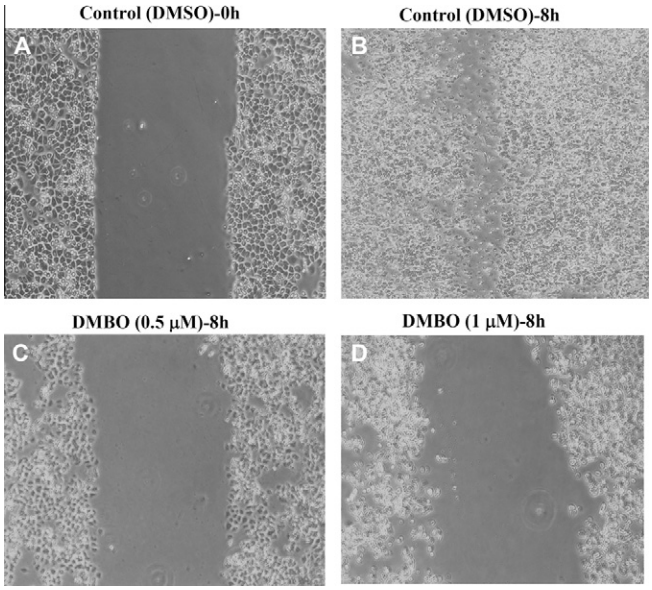

Fig. 7. Effect of DMBO on the migration of UV♀2 cells. The cell monolayers were wounded by scratching, incubated with DMSO (control) or with DMBO (0.5 or 1 μM) in the presence of exogenous VEGF (2 ng/mL) and the wound healing process were photographed digitally with an inverted microscope at 0 h and 8 h.

icity or weight loss during the experiments. To gain further insight into the toxic effects of DMBO (1.5 mg/kg body weight), histological analysis was performed using hematoxylin and eosin (H and E) staining of liver and kidney of both normal and DMBO treated mice. The histological evaluation showed no apparent abnormalities in any DMBO treated mice (Supplemental Fig. 9). Moreover, DMBO failed to show any anti-coagulant activity *in vitro* (data not shown). Heparin (5.0 mg/kg body weight) from porcine intestinal mucosa, a positive control also prevented the increase in liver weight (Fig. 4C) by suppressing the formation of metastatic nodules in the liver.

Further to understand whether DMBO and heparin has synergistic or additive effects, we used the combination of DMBO (0.25 mg/kg body weight) and heparin (2.5 mg/kg body weight) or DMBO (0.5 mg/kg body weight) and heparin (5.0 mg/kg body weight). In LM8G7 cells injected mice, monotherapy with DMBO (0.25 mg/kg body weight) or heparin (2.5 mg/kg body weight) failed to inhibit tumor growth, while combination of DMBO and heparin at the same dosage dramatically enhanced the anti-tumor activity compared with single-agent treatments (Fig. 4C). Treatment of mice with a higher dose of either DMBO (0.5 mg/kg body weight) or heparin (5 mg/kg body weight) alone was able to elicit the same response as compared to the combination of both at the same dosage, suggesting that a synergistic inhibition of tumor growth is evident only at the combined low dose of DMBO (0.25 mg/kg body weight) and heparin (2.5 mg/kg body weight).

3.5. DMBO inhibits human heparanase enzymatic activity in a cell-free system

The heparanase is known to degrade the HS chains specifically [39]. Using FITC-labelled HS as a substrate, we evaluated the ability of DMBO to inhibit heparanase-mediated degradation of HS in a gel-permeation chromatography. The resulting chromatogram revealed that DMBO significantly inhibited the enzymatic activity of human heparanase (Fig. 5A). DMBO strongly and concentration dependently inhibited the heparanase activity with an IC_{50} value of 65 μM (Fig. 5B). In order to know the specificity of DMBO, we also studied the effects of DMBO on hyaluronidase catalytic activity *in vitro* (see Supplemental Experimental Procedures for details). Supplemental Fig. 10 shows the chromatograms of FITC-labelled hyaluronic acid (HA) digested by the hyaluronidase in the presence or absence of DMBO. The enzyme activity of hyaluronidase was not inhibited by the DMBO, indicates that DMBO is not an inhibitor of hyaluronidase. In addition, we also evaluated the effect of DMBO on chondroitinase (CSase) ABC catalytic activity by digesting chondrotin sulfate (CS)-A in the presence or absence of DMBO (see Supplemental Experimental Procedures for details). CSase ABC, digested the CS-A even in the presence of DMBO (Supplemental Fig. 11). These results indicate the specificity of DMBO towards the heparanase.

3.6. Effects of DMBO on the heparan-degrading activity of LM8G7 cells

During metastasis, the activation of a multitude of enzymes/proteins usually occurs. For example, the active secretion of heparanase by tumor cells has been reported [10]. Hence, we determined the effects of DMBO on the heparan-degrading activity of LM8G7 cells. A high level of heparan-degrading activity was detected in LM8G7 cells. The control cell lysates without DMSO (positive control I) or with DMSO (positive control II) degraded the intact HS effectively (Fig. 5C). DMBO at 104 and 206 μM significantly inhibited the degradation of intact HS by 63% and 85% respectively, but DMBO at 55 μM failed to inhibit the heparan-degrading activity (Fig. 5C). Thus, DMBO at higher concentrations significantly abolished the heparan-degrading activity of LM8G7 cells. Therefore, DMBO may prevent the degradation of cell-surface and extracellular HS by heparanase, thereby preventing cancer metastasis.

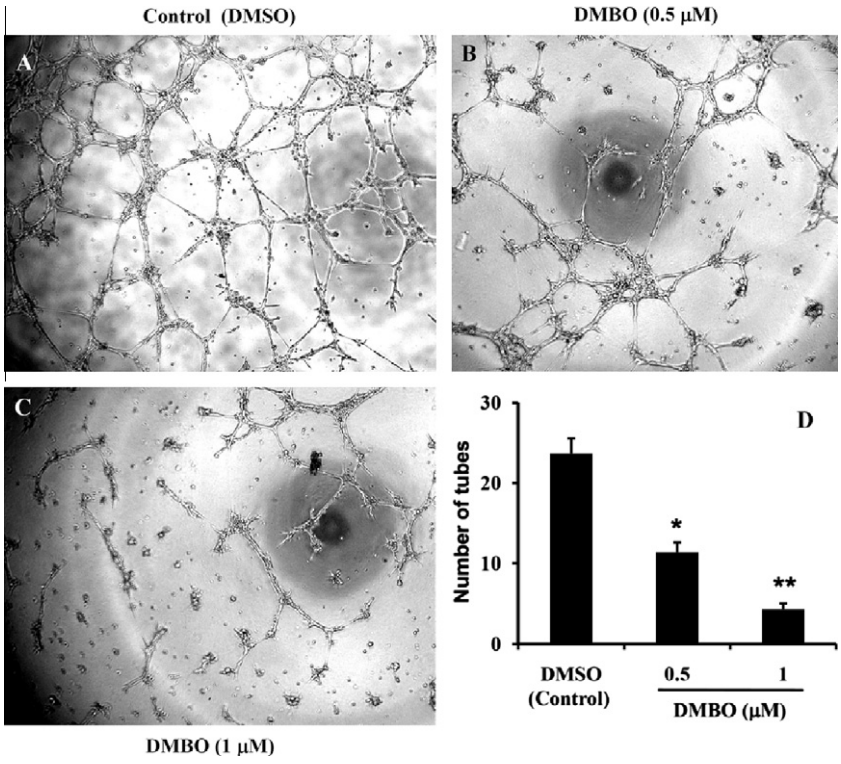

Fig. 8. Effects of DMBO on the tube formation of UV♀2 cells. UV♀2 cells were seeded in ECMatrix™-coated 96-well plates; (A) UV♀2 cells formed the network of intact tubes in 8 h on ECMatrix™ (control). After treatment with 0.5 μM (B), 1.0 μM (C), the tube structures were severely disrupted (magnification 20×) in 8 h on ECMatrix™. (D) Inhibition rates of DMBO on the tube formation of UV♀2 cells. The number of intact tubes were counted in five randomly chosen regions and expressed as the percentage of the control, and the results are expressed as mean ± S.D. $^{*}P < 0.05$ versus control. $^{**}P < 0.01$ versus control. Mann–Whitney *U* test.

3.7. DMBO inhibited the migration and invasion of LM8G7 cells stably expressing VEGF and heparanase

Heparanase expression has been consistently correlated with the metastatic potential of tumor cells. Here, we used the Transwell migration assay to evaluate the effects of DMBO on migration and *in vivo* invasion assay for invasion of LM8G7 cells that stably expresses VEGF and heparanase (Fig. 6A and B). As shown in Fig. 6A and B, the LM8G7 cells abundantly migrated through the filter (without Matrigel coat) or invaded through Matrigel coat (basement membrane material) and passed through the pores to reach the underside of the filter membrane following stimulation with 10% FBS. DMBO at 0.5–5 μM concentrations markedly suppressed the migration and invasion of LM8G7 cells dose-dependently (Fig. 6A and B). These data suggest that the DMBO may inhibit the metastasis of LM8G7 cells to the liver, in part by affecting the migration and invasion of cancer cells.

3.8. DMBO is anti-angiogenic in vitro

Angiogenesis is believed to be mediated by migration, differentiation (tube formation) and proliferation of endothelial cells. Since tumor growth is dependent on angiogenesis, targeting the tumor vasculature makes sense as an anti-tumor strategy [40]. We examined whether DMBO can inhibit VEGF-mediated *in vitro* migration and differentiation of endothelial cells by performing *in vitro* migration and tube formation assays on ECMatrix™ respectively. DMBO selectively inhibited the migration (Fig. 7A–D) and formation of vascular tubes on ECMatrix™ in a dose-dependent manner (Fig. 8A–D). With regard to control, DMBO showed a remarkable suppression of migration and vascular tubes formation, with inhibition rates of 26% and 54% in migration and 52% and 81% in tube formation at 0.5 and 1 μM concentration respectively. Thus DMBO blocked the VEGF-induced migration and tube formation of UV♀2 cells. Interestingly, DMBO does not inhibit FGF-2 induced angiogenesis of UV♀2 cells (data not shown). This observation correlates with our SPR analysis that DMBO showed a weak or no interaction with FGF-2 (Supplementary Fig. 5).

3.9. Effect of DMBO on UV♀2 cells proliferation

The proliferation of endothelial cells to form microvessels is critical for angiogenesis. In fact, inhibition of angiogenic factors mediated proliferation of endothelial cells would be an effective anti-angiogenic therapy and ultimately for cancer prevention. Hence, we tested the effect of DMBO on the VEGF-induced proliferation of endothelial (UV♀2) cells. Markedly, the compound DMBO, strongly bound with VEGF significantly inhibited the VEGF-induced proliferation of UV♀2 cells by 27%, 64%, and 94% at 14, 28 and 59 μM respectively (Fig. 9A). Notably, results shows that compound DMBO suppressed the proliferation of endothelial cells, but the concentration of DMBO and time required to suppress cell proliferation was high compared with that required to suppress the cell migration and tube formation (0.5 and 1 μM). Hence, the inhibitory effect of DMBO on the migration and tube formation could not be attributed to the anti-proliferative activity. Taken together, we demonstrated that DMBO can block the VEGF-mediated angiogenic response on endothelial cells probably by reducing the affinity of VEGF for its receptors on endothelial cells or associated with a significant loss in bioactivity. Further more, the cytotoxic effects of DMBO (2–96 μM) was tested on UV♀2 in the absence of VEGF. Interestingly, after a longer incubation (72 h) of DMBO, in the absence of exogenous VEGF, very less cytotoxicity (Fig 9B) was observed even at higher concentration (96 μM) when compared to cisplatin (10 μM). Taken together, these results show that the anti-proliferative effect of DMBO depends not only on the concentration, but also on the condition of the pathological settings.

3.10. Effects of DMBO or heparin on the proliferation of LM8G7 cells

Numerous studies have shown that overexpression of VEGF, a heparin-binding growth factor, and its receptor plays an important role in tumor-associated angiogenesis and subsequent growth and metastasis [41]. Many sugar-based derivatives have been reported as strong inhibitors of tumor progression and metastasis. However, evidence for the direct binding of small molecules to VEGF is still lacking. Our SPR analysis demonstrated that DMBO directly bound to VEGF probably via non-covalent interactions (Fig. 2B). Further, to support the hypothesis that DMBO

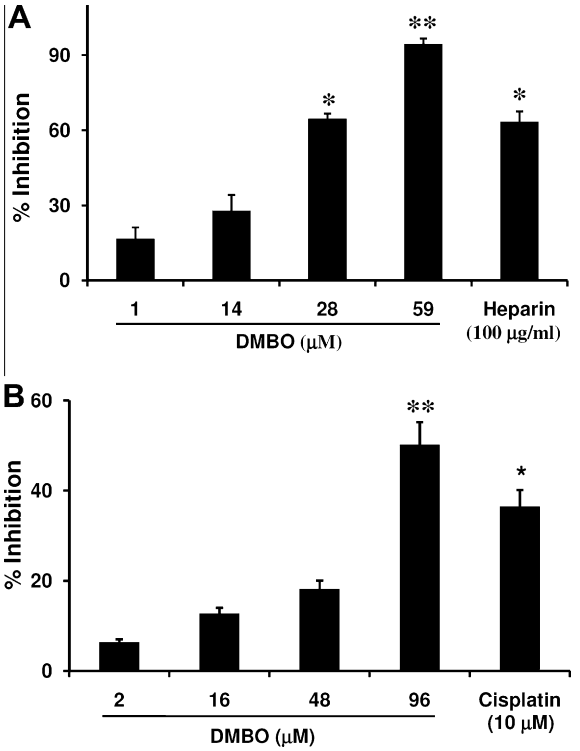

Fig. 9. Effects of DMBO on the proliferation of UV♀2 in the presence or absence of VEGF. (A) UV♀2 cells were cultured overnight and incubated with the indicated concentrations of DMBO (1–59 μM) or heparin (100 μg/mL) in the presence of exogenous VEGF (2 ng/mL) for 48 h. The total number of viable cells was determined and the % inhibition of DMBO against the VEGF-induced proliferation of UV♀2 cells is presented. (B) % Inhibition of DMBO against the proliferation of UV♀2 cells in the absence of VEGF. UV♀2 cells were cultured overnight and incubated with the indicated concentrations of DMBO (2–96 μM) or cisplatin (10 μM). The total number of viable cells was determined and the % inhibition of DMBO against the proliferation of UV♀2 cells was presented. Data represent the mean values ± S.D. for four identical wells from three independent experiments. $^{*}P < 0.05$ versus control. $^{**}P < 0.01$ versus control. Mann–Whitney *U* test.

may also act through growth factor mediated cell signalling, we analyzed the effects of DMBO or heparin on the proliferation of LM8G7 cells in the presence of various concentration of exogenous VEGF. As expected, addition of exogenous VEGF seems to promote the proliferation of LM8G7 cells to some extend in an autocrine manner. Presence of excess exogenous VEGF partially counteracted the anti-proliferative effects of DMBO on the LM8G7 cells (Fig. 10A). These observations suggest that DMBO may bind with VEGF and thereby inhibit the mitogenic effects of VEGF on the proliferation of LM8G7 cells, but the exact mechanism is still not obvious. Further, the synergistic effect of DMBO and heparin on the proliferation of LM8G7 cells was studied by using DMBO (25 or 50 μM) alone and heparin (25 or 50 μg/mL) alone or in combination of DMBO (25 or 50 μM) with heparin (25 or 50 μg/mL). The proliferation of LM8G7 cells was strongly inhibited in combination of both DMBO and heparin. (Fig. 10B). Our data have provided evidence that a synergistic anti-proliferative effect was observed when DMBO combined with heparin and these results are consistent with the *in vivo* anti-tumor effect.

4. Conclusion

Although we have synthesized many oxazine derivatives that bear the same nucleus as that of DMBO, to the best of our knowledge, this is the first report on a synthetic oxazine that appears to mimic functional groups and pyranosidic ring

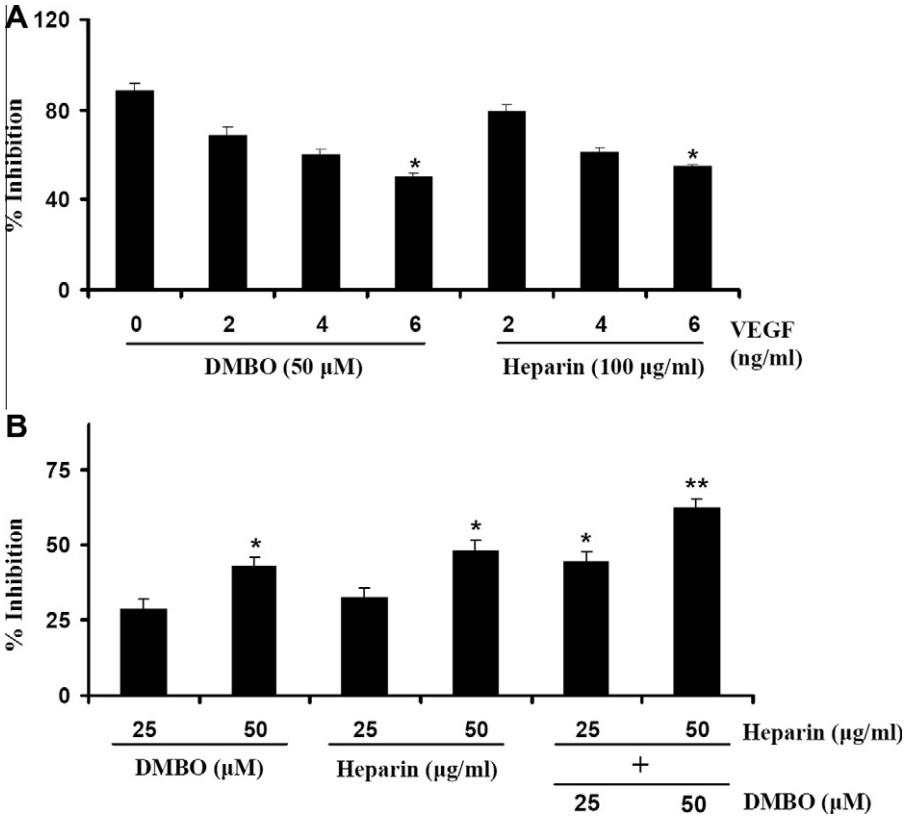

Fig. 10. Effects of DMBO and heparin on the proliferation LM8G7 cells. (A) LM8G7 cells were cultured overnight and incubated with DMBO (50 μM) or heparin (100 μg/mL) in the presence of various concentrations of VEGF (2–6 ng/mL) for 48 h. The total number of viable cells was determined and the % inhibition of DMBO (50 μM) or heparin (100 μg/mL) against the VEGF-induced proliferation of LM8G7 cells is presented. (B) Synergistic anti-proliferative effect of DMBO with heparin on LM8G7 cells. LM8G7 cells were cultured overnight and incubated with DMBO (25 or 50 μM) alone and heparin (25 or 50 μg/mL) alone or in combination of DMBO (25 or 50 μM) with heparin (25 or 50 μg/mL) for 48 h. The total number of viable cells was determined and the % inhibition of DMBO or the synergistic effect of DMBO and heparin against the proliferation of LM8G7 cells is presented. Data represent the mean values ± S.D. for four identical wells from three independent experiments. $^{*}P < 0.05$ versus control. $^{**}P < 0.01$ versus control. Mann–Whitney *U* test.

structure of HS, interacts directly with growth factors/cytokines with high affinity. Thus, we propose that DMBO binds VEGF and might effectively block the ability of VEGF to activate its receptor and its further signalling. Further, the *in vivo* anti-metastatic mechanism of DMBO on LM8G7 cells lies greatly in its ability to interrupt heparanase-associated pathologic events and this effect is most important and comparable to other sugar mimetic anti-metastatic agents [42].

In addition, DMBO inhibited the catalytic activity of heparanase. Also, DMBO may block the VEGF-mediated angiogenic responses *in vitro* on endothelial cells. Thus, DMBO anti-tumor activity could be attributed at least in part, by modulating the early and late steps of metastasis involving tumor and endothelial cell functions. Evidently, DMBO showed an anti-tumor effect with heparin synergistically in osteosarcoma model. However, additional studies are needed to elucidate the detailed mechanism of action of DMBO to develop new carbohydrate-mimetic-based cancer therapeutic molecules.

Conflict of interest

The authors do not have any conflicts of interest to report with for this manuscript.

Acknowledgments

This work was supported in part by the Indian National Science Academy (INSA)–Japan Society for the Promotion of Science (JSPS) program between India (to K.S.R.) and Japan (to K.S.), and a Grant-in-aid (19-07194) from JSPS. This work was also supported in part by the Future Drug Discovery and Medical Care Innovation Program (K.S.) from the Ministry of Education, Culture, Sports, Science, and Technology of Japan (MEXT). We thank Prof. Miyasaka M. for providing the LM8G7 cells. We also thank Prof. Osada H., Dr. Kondoh Y., and Dr. Akiko S. for providing the SPR imaging data.

Appendix A. Supplementary material

Supplementary data associated with this article can be found, in the online version, at doi:10.1016/j.canlet.2010.05.016.

References

[1] R. Henriksson, K. Grankvist, Interactions between anticancer drugs and other clinically used pharmaceuticals. A review, Acta Oncol. 28 (1989) 451–462.

[2] B. Weidmann, R.H. Abeles, Mechanism of inactivation of chymotrypsin by 5-butyl-3H-1,3-oxazine-2,6-dione, Biochemistry 23 (1984) 2373–2376.
[3] Y. Kusakabe, J. Nagatsu, M. Shibuya, O. Kawaguchi, C. Hirose, Minimycin, a new antibiotic, J. Antibiot. 25 (1972) 44–47.
[4] A.R. Moorman, R.H. Abeles, New class of serine protease inactivators based on isatoic anhydride, J. Am. Chem. Soc. 104 (1982) 6785–6786.
[5] C. Mundhenke, K. Meyer, S. Drew, A. Friedl, Heparan sulfate proteoglycans as regulators of fibroblast growth factor-2 receptor binding in breast carcinomas, Am. J. Pathol. 160 (2002) 185–194.
[6] R.V. Iozzo, J.D. San Antonio, Heparan sulfate proteoglycans: heavy hitters in the angiogenesis arena, J. Clin. Invest. 108 (2001) 349–355.
[7] C.L. Chu, A.L. Goerges, M.A. Nugent, Identification of common and specific growth factor binding sites in heparan sulfate proteoglycans, Biochemistry 44 (2005) 12203–12213.
[8] I. Vlodavsky, R. Bar-Shavit, R. Ishai-Michaeli, P. Bashkin, Z. Fuks, Extracellular sequestration and release of fibroblast growth factor: a regulatory mechanism?, Trends Biochem Sci. 16 (1991) 268–271.
[9] I. Vlodavsky, Y. Friedmann, M. Elkin, H. Aingorn, R. Atzmon, R. Ishai-Michaeli, M. Bitan, O. Pappo, T. Peretz, I. Michal, L. Spector, I. Pecker, Mammalian heparanase: gene cloning, expression and function in tumor progression and metastasis, Nat. Med. 5 (1999) 793–802.
[10] O. Goldshmidt, E. Zcharia, R. Abramovitch, S. Metzger, H. Aingorn, Y. Friedmann, V. Schirrmacher, E. Mitrani, I. Vlodavsky, Cell surface expression and secretion of heparanase markedly promote tumor angiogenesis and metastasis, Proc. Natl. Acad. Sci. USA 99 (2002) 10031–10036.
[11] M.D. Hulett, C. Freeman, B.J. Hamdorf, R.T. Baker, M.J. Harris, C.R. Parish, Cloning of mammalian heparanase, an important enzyme in tumor invasion and metastasis, Nat. Med. 5 (1999) 803–809.
[12] R. Sasisekharan, Z. Shriver, G. Venkataraman, U. Narayanasami, Roles of heparan–sulphate glycosaminoglycans in cancer, Nat. Rev. Cancer 2 (2002) 521–528.
[13] K. Ishida, M.K. Wierzba, T. Teruya, S. Simizu, H. Osada, Novel heparan sulfate mimetic compounds as antitumor agents, Chem. Biol. 11 (2004) 367–377.
[14] D.G. Jayne, S.L. Perry, E. Morrison, S.M. Farmery, P.J. Guillou, Activated mesothelial cells produce heparin-binding growth factors: implications for tumor metastases, Br. J. Cancer 82 (2000) 1233–1238.
[15] T. Tammela, G. Zarkada, E. Wallgard, A. Murtomäki, S. Suchting, M. Wirzenius, M. Waltari, M. Hellström, T. Schomber, R. Peltonen, C. Freitas, A. Duarte, H. Isoniemi, P. Laakkonen, G. Christofori, S. Ylä-Herttuala, M. Shibuya, B. Pytowski, A. Eichmann, C. Betsholtz, K. Alitalo, Blocking VEGFR-3 suppresses angiogenic sprouting and vascular network formation, Nature 454 (2008) 656–660.
[16] T. Cohen, H. Gitay-Goren, R. Sharon, M. Shibuya, R. Halaban, B.Z. Levi, G. Neufeld, $VEGF_{121}$, a vascular endothelial growth factor (VEGF) isoform lacking heparin binding ability, requires cell-surface heparin sulfates for efficient binding to the VEGF receptors of human melanoma cells, J. Biol. Chem. 270 (1995) 11322–11326.
[17] S. Miyamoto, M. Hirata, A. Yamanaki, T. Kageyama, H. Hasuwa, H. Mizushima, Y. Tanaka, H. Yagi, K. Sonoda, M. Kai, H. Kanoh, H. Nakano, E. Mekada, Heparin-binding EGF-like growth factor is a promising target for ovarian cancer therapy, Cancer Res. 64 (2004) 5720–5727.
[18] D.B. Ramnarain, S. Park, D.Y. Lee, K.J. Hatanpaa, S.O. Scoggin, H. Out, T.A. Libermann, J.M. Raisanen, R. Ashfaq, E.T. Wong, J. Wu, R. Elliott, A.A. Habib, Differential gene expression analysis reveals generation of an autocrine loop by a mutant epidermal growth factor receptor in glioma cells, Cancer Res. 66 (2006) 867–874.
[19] J. Kim, W.J. Jahng, D. Di Vizio, J.S. Lee, R. Jhaveri, M.A. Rubin, A. Shisheva, M.R. Freeman, The phosphoinositide kinase PIKfyve mediates epidermal growth factor receptor trafficking to the nucleus, Cancer Res. 67 (2007) 9229–9237.
[20] S. Miyamoto, H. Yagi, F. Yotsumoto, T. Kawarabayashi, E. Mekada, Heparin-binding epidermal growth factor-like growth factor as a novel targeting molecule for cancer therapy, Cancer Sci. 97 (2006) 341–347.
[21] J.H. Egberts, V. Cloosters, A. Noack, B. Schniewind, L. Thon, S. Klose, B. Kettler, C. von Forstner, C. Kneitz, J. Tepel, D. Adam, H. Wajant, H. Kalthoff, A. Trauzold, Anti-tumor necrosis factor therapy inhibits pancreatic tumor growth and metastasis, Cancer Res. 68 (2008) 1443–1450.
[22] C.M. Lee, T. Tanaka, T. Murai, M. Kondo, J. Kimura, W. Su, T. Kitagawa, T. Ito, H. Matsuda, M. Miyasaka, Novel chondroitin sulfate-binding cationic liposomes loaded with cisplatin efficiently suppress the local growth and liver metastasis of tumor cells in vivo, Cancer Res. 62 (2002) 4282–4288.
[23] I.J. Fidler, G.L. Nicolson, Organ selectivity for implantation survival and growth of B16 melanoma variant tumor lines, J. Natl. Cancer Inst. 57 (1976) 1199–1202.
[24] Basappa, S. Murugan, K.N. Sugahara, C.M. Lee, G.B. ten Dam, T.H. van Kuppevelt, M. Miyasaka, S. Yamada, K. Sugahara, Involvement of chondroitin sulfate E in the liver tumor focal formation of murine osteosarcoma cells, Glycobiology 19 (2009) 735–742.
[25] J.Z. Xing, L. Zhu, J.A. Jackson, S. Gabos, X.J. Sun, X.B. Wang, X. Xu, Dynamic monitoring of cytotoxicity on microelectronic sensors, Chem. Res. Toxicol. 18 (2005) 154–161.
[26] Y. Okada, S. Yamada, M. Toyoshima, J. Dong, M. Nakajima, K. Sugahara, Structural recognition by recombinant human heparanase that plays critical roles in tumor metastasis. Hierarchical sulfate groups with different effects and the essential target disulfated trisaccharide sequence, J. Biol. Chem. 277 (2002) 42488–42495.
[27] H. Takahashi, S. Ebihara, T. Okazaki, S. Suzuki, M. Asada, H. Kubo, H. Sasaki, Design and synthesis of a heparanase inhibitor with pseudodisaccharide structure, Lung Cancer 45 (2004) 207–214.
[28] C. Fernández, C.M. Hattan, R.J. Kerns, Semi-synthetic heparin derivatives: chemical modifications of heparin beyond chain length, sulfate substitution pattern and N-sulfo/N-acetyl groups, Carbohyd. Res. 341 (2006) 1253–1265.
[29] H.Q. Miao, M. Elkin, E. Aingorn, R. Ishai-Michaeli, C.A. Stein, I. Vlodavsky, Inhibition of heparanase activity and tumor metastasis by laminarin sulfate and synthetic phosphorothioate oligodeoxynucleotides, Int. J. Cancer 83 (1999) 424–431.
[30] I. Saiki, J. Murata, M. Nakajima, S. Tokura, I. Azuma, Inhibition by sulfated chitin derivatives of invasion through extracellular matrix and enzymatic degradation by metastatic melanoma cells, Cancer Res. 50 (1990) 3631–3637.
[31] V. Ferro, K. Dredge, L. Liu, E. Hammond, I. Bytheway, C. Li, K. Johnstone, T. Karoli, K. Davis, E. Copeman, A. Gautam, PI-88 and novel heparan sulfate mimetics inhibit angiogenesis, Semin. Thromb. Hemost. 33 (2007) 557–568.
[32] S. Takahashi, H. Kuzuhara, M. Nakajima, Design and synthesis of a heparanase inhibitor with pseudodisaccharide structure, Tetrahedron 57 (2001) 6915–6926.
[33] Basappa, C.V. Kavitha, K.S. Rangappa, Simple and an efficient method for the synthesis of 1-[2-dimethylamino-1-(4-methoxyphenyl)-ethyl]-cyclohexanol hydrochloride: (+/−) venlafaxine racemic mixtures, Bioorg. Med. Chem. Lett. 14 (2004) 3279–3281.
[34] C.V. Kavitha, S. Lakshmi, Basappa, K. Mantelingu, M.A. Sridhar, J. Prasad, K.S. Rangappa, Synthesis and molecular structure analysis of venlafaxine intermediate and its analog, J. Chem. Cryst. 35 (2006) 957–963.
[35] A. Saito, K. Kawai, H. Takayama, T. Sudo, H. Osada, Improvement of photoaffinity SPR imaging platform and determination of binding site of p62/SQSTM1 to p38 MAP kinase, Chem. Asian J. 3 (2008) 1607–1612.
[36] F. Kratz, Albumin as a drug carrier: design of prodrugs, drug conjugates and nanoparticles, J. Control Release 132 (2008) 171–183.
[37] T. Waldman, Y. Zhang, L. Dillehay, J. Yu, K. Kinzler, B. Vogelstein, Williams, Cell-cycle arrest versus cell death in cancer therapy, J. Nat. Med. 3 (1997) 1034–1036.
[38] A.F. Chambers, The metastatic process: basic research and clinical implications, Oncol. Res. 11 (1999) 161–168.
[39] D.S. Pikas, J.P. Li, I. Vlodavsky, U. Lindahl, Substrate specificity of heparanases from human hepatoma and platelets, J. Biol. Chem. 273 (1998) 18770–18777.
[40] M. Dhanabal, M. Jeffers, W.J. Larochelle, Anti-angiogenic therapy as a cancer treatment paradigm, Curr. Med. Chem. Anticancer Agents 5 (2005) 115–130.
[41] Z. Zhu, L. Witte, Inhibition of tumor growth and metastasis by targeting tumor-associated angiogenesis with antagonists to the receptors of vascular endothelial growth factor, Invest. New Drugs 17 (1999) 195–212.
[42] H. Zhao, H. Liu, Y. Chen, X. Xin, J. Li, Y. Hou, Z. Zhang, X. Zhang, C. Xie, M. Geng, J. Ding, Oligomannurarate sulfate, a novel heparanase inhibitor simultaneously targeting basic fibroblast growth factor, combats tumor angiogenesis and metastasis, Cancer Res. 66 (2006) 8779–8887.